Flow regimes and parameter dependence in nanochannel flows

Chong Liu and Zhigang Li
Department of Mechanical Engineering, The Hong Kong University of Science and Technology, Clear Water Bay, Kowloon, Hong Kong
(Received 9 March 2009; revised manuscript received 30 June 2009; published 1 September 2009)

Nanoscale fluid flow systems involve both microscopic and macroscopic parameters, which compete with each another and lead to different flow regimes. In this work, we investigate the interactions of four fundamental parameters, including the fluid-fluid, fluid-wall binding energies, temperature of the system, and driving force, and their effects on the flow motion in nanoscale Poiseuille flows. By illustrating the fluid flux as a function of a dimensionless number, which represents the effective surface effect on the fluid, we show that the fluid motion in nanochannels falls into different regimes, each of which is associated with a distinct mechanism. The mechanisms in different situations reveal the effects of the parameters on the fluid dynamics.

DOI: 10.1103/PhysRevE.80.036302 PACS number(s): 47.61.−k

The potential applications of nanofluidics in science and engineering have motivated intensive investigations of fluid flow in nanochannels, where the classical Navier-Stokes (NS) equations may not apply. Some microscopic parameters that are not considered in the classical treatments play important roles in nanoscale fluid flows, such as the molecular binding energies for the fluid-fluid and fluid-surface interactions [1,2]. These microscopic parameters are directly related to some macroscopic variables, including the temperature and external driving force of the flow system. The temperature of the system measures the thermal vibration of the fluid molecules, which can break the fluid-surface binding if the temperature is high [1,3,4]. Similarly, a large driving force can help fluid molecules overcome the attraction of the surface [5–8]. On the other hand, the competition between fluid-fluid and fluid-surface binding energies becomes critical when the temperature is low and the driving force is small [2,7,9]. The coupling of these parameters at different scales determines the flow regimes, where the mechanisms of how the parameters affect the fluid motion are different. For both theoretical analysis and practical applications, it is essential to probe the flow regimes and the parameter dependence in nanochannel flows.

Over the past two decades, many attempts have been made to understand the behavior of confined fluids in the nanoscale, including static and dynamic properties as well as boundary conditions [10–21]. Many attentions were focused on how surfaces affect the fluid motion through molecular interactions [4–8,16–21]. It has been well known that strong fluid-wall binding energy $\varepsilon_{\mathrm{fw}}$ favors fluid adsorption on the wall surface and stick boundary condition tends to be valid in this case [1,4,5,9,11,17]. The temperature of the system T is another factor that affects fluid adsorption and the ratio $\varepsilon_{\mathrm{fw}}/kT$ is usually used to predict the adsorption, where k is the Boltzmann constant. However, $\varepsilon_{\mathrm{fw}}/kT$ may not be sufficient to describe the behavior of fluids at the surface. Many other parameters, such as the external driving force and fluid density, also affect the fluid properties at the interface [15,16,18,21,22]. Furthermore, the molecular binding energy among fluid molecules $\varepsilon_{\mathrm{ff}}$ competes with the fluid-wall binding $\varepsilon_{\mathrm{fw}}$ and can be important in certain conditions. These interacting parameters bring about different flow regimes and cause the analysis of nanoscale fluid motion more complicated than the classical treatments. How these parameters affect the fluid motion becomes a critical issue in understanding the behavior of fluids in nanoconfinements. Among these parameters, the fluid-fluid ($\varepsilon_{\mathrm{ff}}$) and fluid-wall ($\varepsilon_{\mathrm{fw}}$) binding energies, temperature of the system T, and external driving force F_e are the representative and key parameters. Although the roles of some of the parameters have been studied in literature, a clear picture about how they are coupled and the consequent flow regimes requires further explorations.

In this work, we investigate the interactions among the aforementioned four parameters, $\varepsilon_{\mathrm{ff}}$, $\varepsilon_{\mathrm{fw}}$, T, and F_e and the corresponding flow regimes. Nanoscale planar Poiseuille flows are studied by using nonequilibrium molecular-dynamics (NEMD) simulations. We show that the fluid motion can be classified into different regimes if it is properly illustrated. The mechanisms that govern the fluid behavior in the regimes offer a general picture of how these four parameters interact with each another and affect the dynamics of fluids in nanochannels.

The Poiseuille flow system considered in this work, similar to that in Ref. [3], consists of two parallel planar Ag walls with a liquid in between. The tight-binding potential function is used to consider the thermal vibrations of the wall atoms [3], which affect the energy accommodation of the wall and the dynamics of fluid molecules at the wall surface [1,9]. The fluid is modeled by the Lennard-Jones (LJ) potential, $U(r)=4\varepsilon[(\sigma/r)^{12}-(\sigma/r)^{6}]$, where r is the separation between a pair of molecules, σ is the collision diameter, and ε is the binding energy. Since the self-binding energy for many popular fluids $\varepsilon_{\mathrm{ff}}$ is less than or of the order of room temperature, we shall use liquid Ar ($\varepsilon_{\mathrm{ff}}=114$ K) as a representative fluid. Liquid He ($\varepsilon_{\mathrm{ff}}=10$ K) is employed to represent light species [23]. The LJ potential is also used to calculate the interactions between the fluid molecules and wall atoms. The basic units, the length, mass, and energy, in the NEMD simulations are set to be Angstrom, the mass of one Ag atom, and eV, respectively. To examine the role of fluid-wall interaction, we artificially change the fluid-wall binding energy $\varepsilon_{\mathrm{fw}}$ in a wide range. The temperature of the system is maintained at a certain value by applying the Berendsen thermostat to the walls [24]. The potential is truncated at 10.21 Å and Newton's equations are integrated with Beeman's leap-frog algorithm, with time step equal to 1 fs [1,3]. Different channel sizes, from about 2 to 4 nm between the two walls (y

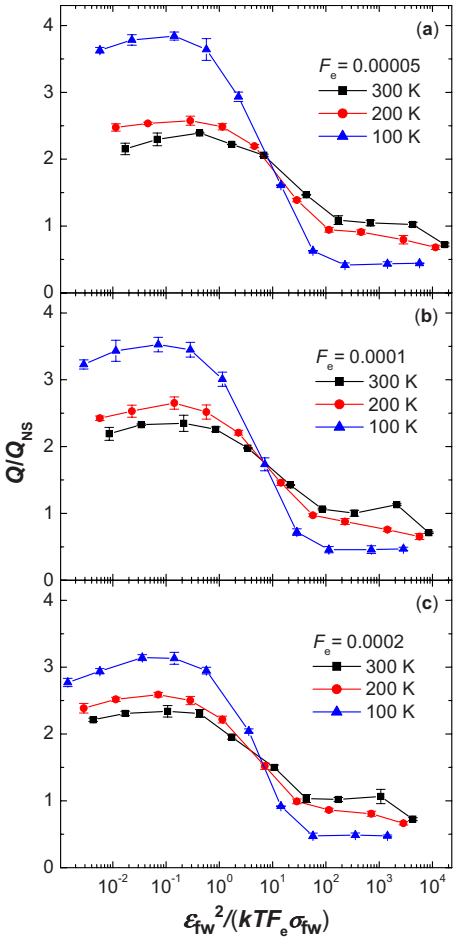

FIG. 1. (Color online) The reduced mass flux of liquid Ar as a function of $\varepsilon_{\mathrm{fw}}^2/(kTF_e\sigma_{\mathrm{fw}})$ in a channel of 3.7 nm for different temperatures and external forces. The external forces F_e (corresponding pressure drops along the channel) on each fluid molecule are (a) 5×10^{-5} (33 MPa), (b) 1×10^{-4} (66 MPa), and (c) 2×10^{-4} (132 MPa).

direction), are used and the dimensions in the x and z directions are 19.8 and 4.9 nm. Periodic boundary conditions are employed in the x and z directions only. An external force is applied to each fluid molecule in the x direction, which is increased linearly with time until the desired value is reached. All the actions and measurements are made after equilibration and the details can be found in Ref. [3].

There is no doubt that the boundary condition, say, slip length, at the fluid-wall interface is an important issue in understanding the fluid-wall interaction. However, to understand the flow regimes and the relations of many parameters at different scales, the slip length may not be a suitable quantity. In this work, we shall examine the flow flux. As will be shown later, there are several clear regimes for the fluid motion when the fluid flux is plotted as a function of a dimensionless number, which represents the effective surface effect.

To understand how the parameters interact, one approach is to observe certain quantities (e.g., flow rate) by varying only one of the variables at a time. This is tedious and sometimes practically impossible. Well-designed dimensionless

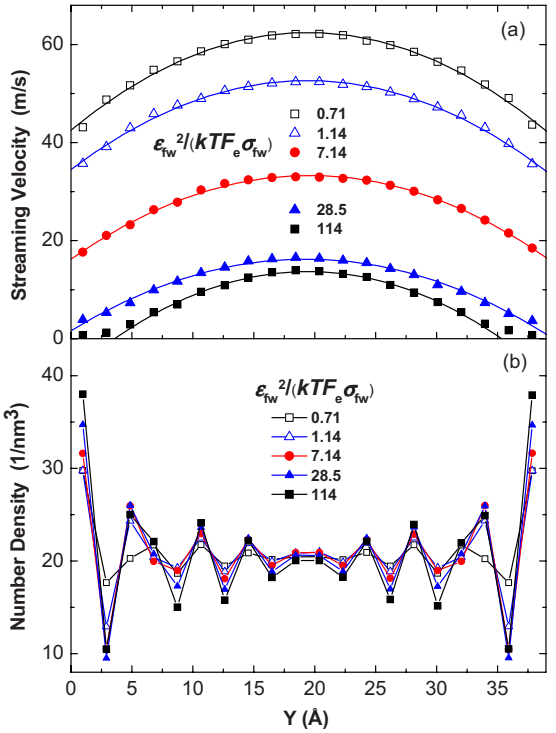

FIG. 2. (Color online) (a) Velocity and (b) density distributions of liquid Ar in the channel at different values of $\varepsilon_{\mathrm{fw}}^2/(kTF_e\sigma_{\mathrm{fw}})$ for the case of $T=100$ K and $F_e=1\times10^{-4}$. Solid lines in (a) are the parabolic fits shifted by the slip velocities.

numbers, which contain information about the competition of some parameters, can greatly simplify the analysis. It is known that strong fluid-wall binding energy $\varepsilon_{\mathrm{fw}}$ and low temperature kT favor the fluid adsorption on the wall surface. Therefore, $\varepsilon_{\mathrm{fw}}/kT$ is an appropriate dimensionless number for understanding the surface effect on the fluid. In Poiseuille flows, the fluid-wall binding force, $F_{\mathrm{fw}}=-\partial U/\partial r$, and the external driving force F_e form another competition. If the average binding force $\bar{F}_{\mathrm{fw}}$ is approximated as the force evaluated at the separation $r=\sigma_{\mathrm{fw}}$, where the potential vanishes, $\bar{F}_{\mathrm{fw}}\sim\varepsilon_{\mathrm{fw}}/\sigma_{\mathrm{fw}}$. Therefore, the dimensionless number $\varepsilon_{\mathrm{fw}}/(F_e\sigma_{\mathrm{fw}})$ bears similar physical meaning to $\varepsilon_{\mathrm{fw}}/kT$ and can be equally important. Since both $\varepsilon_{\mathrm{fw}}/kT$ and $\varepsilon_{\mathrm{fw}}/(F_e\sigma_{\mathrm{fw}})$ indicate the relative binding strength between the fluid and wall, their product $\varepsilon_{\mathrm{fw}}^2/(kTF_e\sigma_{\mathrm{fw}})$ can be a sensitive indicator for the effective surface effect on the fluid. We shall use this dimensionless number to study the fluid flux.

We first measure the mass flux Q of liquid Ar in channels of 3.7 nm between the walls under different temperatures and external forces. The LJ parameters for Ar are taken as $\varepsilon_{\mathrm{ff}}=114$ K and $\sigma_{\mathrm{ff}}=3.47$ Å [3,23]. The fluid-wall binding energy $\varepsilon_{\mathrm{fw}}$ is varied to cover a wide range, while σ_{fw} is kept constant. Figure 1 shows the reduced mass flux Q/Q_{NS} as a function of $\varepsilon_{\mathrm{fw}}^2/(kTF_e\sigma_{\mathrm{fw}})$, where Q_{NS} is the prediction of the NS equations at the boiling point at 1 atm. The corresponding pressure drops over the channel for the external forces, 5×10^{-5}, 1×10^{-4}, and 2×10^{-4} in Figs. 1(a)–1(c) are 33, 66, and 132 MPa. For each external force, the flux is measured at three different temperatures, 100, 200, and 300 K. It is seen

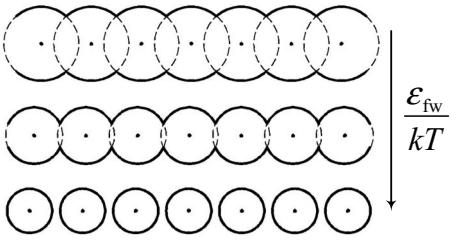

FIG. 3. The schematic of equipotential surfaces, which represent the real wall surface. The strength of the fluid-wall interaction decreases from the top to bottom panel.

that there is a critical value at $\varepsilon_{fw}^2/(kTF_e\sigma_{fw}) \approx 7$, which divides the flow into two regimes. The mechanism of how the temperature affects the flux is completely different in these two regimes. Before the critical value, let us call it regime I, the flux decreases as the temperature increases for a given value of $\varepsilon_{fw}^2/(kTF_e\sigma_{fw})$. However, the flux increases with increasing temperature when $\varepsilon_{fw}^2/(kTF_e\sigma_{fw})$ is larger than the critical value (regime II). The critical value is a division point of strong and weak fluid-wall interactions. In regime I, the surface effect is relatively weak and no fluid adsorption is

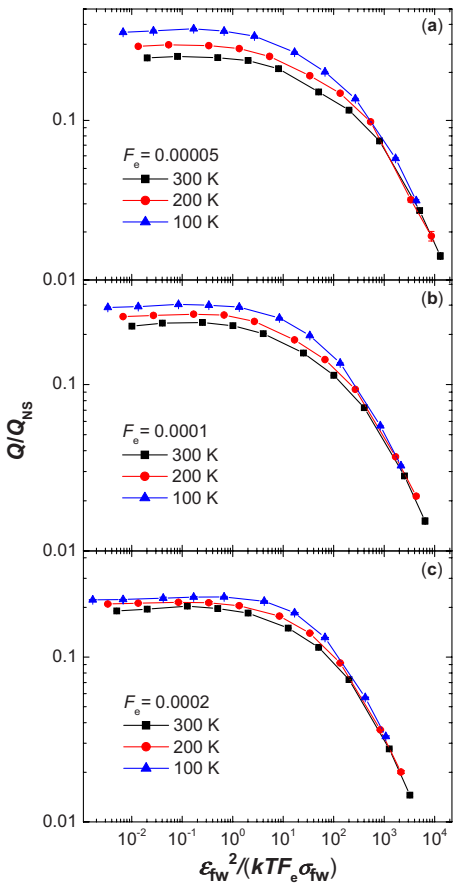

FIG. 4. (Color online) The reduced mass flux of liquid He as a function of $\varepsilon_{fw}^2/(kTF_e\sigma_{fw})$ for different temperatures and external forces. The channel size is 3.7 nm and the external forces F_e (corresponding pressure drops along the channel) on each fluid molecule are (a) 5×10^{-5} (30 MPa), (b) 1×10^{-4} (59 MPa), and (c) 2×10^{-4} (120 MPa).

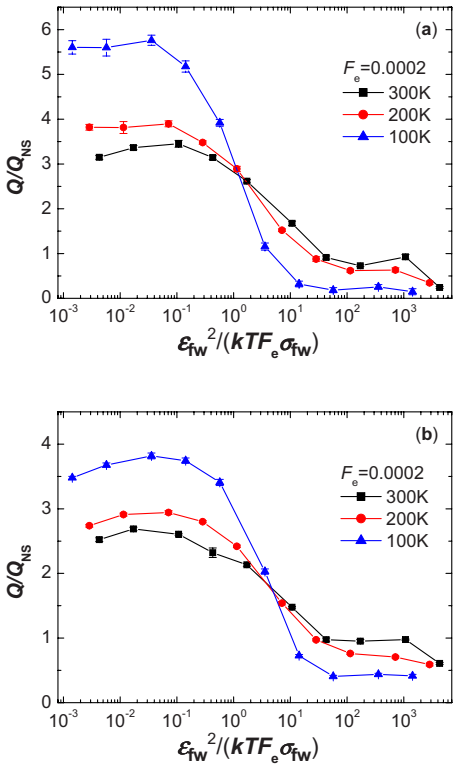

FIG. 5. (Color online) The reduced mass flux of liquid Ar in channels of (a) 1.8 nm and (b) 2.8 nm.

observed, as indicated by the velocity and density profiles in Fig. 2. In this case, when the temperature is raised, the thermal motions of the fluid molecules are enhanced, which increase the collision frequency between the fluid and wall and consequently the friction at the interface. Therefore, the flux, in this regime, is dominated by the temperature-induced friction between the fluid and wall. In regime II, however, as $\varepsilon_{fw}^2/(kTF_e\sigma_{fw})$ is increased, the surface effect on the fluid grows strong and fluid adsorption tends to take place. This can be confirmed by the decreasing fluid slip and increasing fluid density close to the wall surface, as shown in Fig. 2 [25]. In this regime, a high temperature helps the fluid molecules free themselves from the adsorbed layers and join the main flow stream of the fluid. This explains why the flux increases when the temperature is increased. It is noted that the relation of these parameters is not clear if the boundary condition (e.g., slip length) is illustrated (not reported here). It is also noted that the velocity profiles can be well represented by the classical parabolic profiles corrected by the slip velocities if the fluid-wall interaction is not very strong [Fig. 2(a)]. However, this does not mean that the slip-corrected classical approach can predict the flux of nanochannel flows because the density and viscosity of the confined fluid are nonuniform [3,20]. For instance, the volumetric flux of the flow with $\varepsilon_{fw}^2/(kTF_e\sigma_{fw})=28.5$ in Fig. 2 is equal to 11.7 m/s if the slip-corrected parabolic velocity profile is used, while the flux given by the MD simulation is equal to 9.7 m/s. The discrepancy is due to the fact that the fluid density close to the wall is much larger than that in the center area, as shown in Fig. 2(b).

In Fig. 1, it is also seen that the flux generally decreases

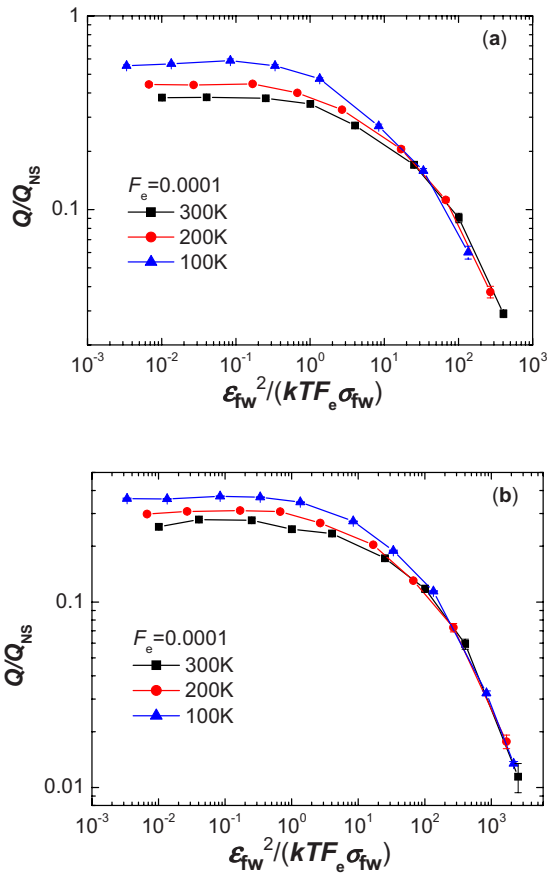

FIG. 6. (Color online) The reduced mass flux of liquid He in channels of (a) 1.8 nm and (b) 2.8 nm (b).

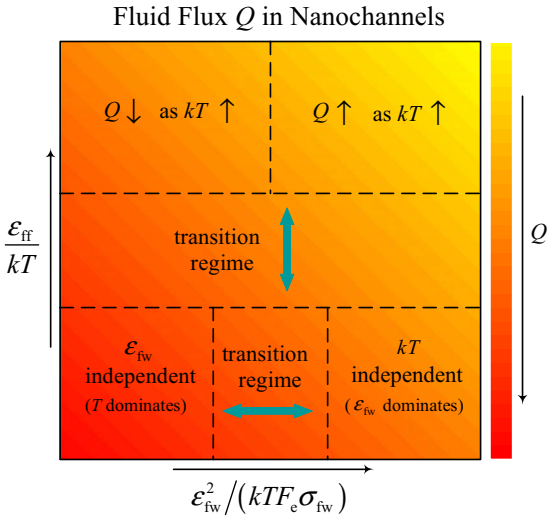

FIG. 7. (Color online) Flow regimes in $\varepsilon_{ff}/kT-\varepsilon_{fw}^2/(kTF_e\sigma_{fw})$ plane in terms of mass flux. The background color saturation indicates the qualitative dependence of flux on the parameters.

as $\varepsilon_{fw}^2/(kTF_e\sigma_{fw})$ increases in regime II. This is due to the fact that the number of fluid molecules in the main stream drops when the molecules tend to be adsorbed by the wall with increasing fluid-wall interaction. In regime I, there is a maximum in the flux as $\varepsilon_{fw}^2/(kTF_e\sigma_{fw})$ changes. To explain the maximum, it is necessary to look into the "real" wall surface, with which the fluid molecules interact. For the fluid-wall interaction, a large binding energy corresponds to a strong repulsive force at small separations, which prevents the fluid molecule from getting close to the wall. The real wall surface for the fluid molecules can be represented by an equipotential surface, beyond which no fluid molecules can pass. Figure 3 sketches such equipotential surfaces at different binding energies ε_{fw}. In Fig. 3, the dots are the centers of wall atoms and the solid curves and circles denote the equipotential surfaces. For very small ε_{fw}/kT, it is seen that fluid molecules can be very close to and even penetrate into the wall. In this case, the surface of the wall is rough and the friction at the interface is large. If ε_{fw}/kT is relatively large, the atomic wall surface becomes smooth and the friction decreases. Hence, in regime I, when $\varepsilon_{fw}^2/(kTF_e\sigma_{fw})$ is very small, the friction caused by the rough atomic surface dominates over the fluid-wall attraction. As $\varepsilon_{fw}^2/(kTF_e\sigma_{fw})$ increases, the increasing smoothness of the surface reduces the friction and the flux goes up. At relatively large $\varepsilon_{fw}^2/(kTF_e\sigma_{fw})$, the fluid-wall interaction starts to be a major factor, which increases the friction and reduces the flux by strong attractive force between the fluid and wall.

For Ar, the fluid-fluid self-binding energy $\varepsilon_{ff}/kT\sim 1$. For some light species, ε_{ff} is small and $\varepsilon_{ff}/kT\ll 1$. To explore the flow regimes and the interactions of the parameters at weak ε_{ff}, we replace Ar by liquid He, for which $\varepsilon_{ff}=10$ K and $\varepsilon_{ff}/kT\sim 0.1$ [23]. The reduced flux for He in the same channel is plotted in Fig. 4. For He, it is seen that there does not exist a critical value for $\varepsilon_{fw}^2/(kTF_e\sigma_{fw})$. In contrast, there are three different regimes. When $\varepsilon_{fw}^2/(kTF_e\sigma_{fw})$ is very small, the flux decreases as increasing temperature. This is the same as that for Ar. Furthermore, the flux is generally independent of ε_{fw}, which indicates that the temperature, in this regime, dominates over ε_{fw}. However, for large $\varepsilon_{fw}^2/(kTF_e\sigma_{fw})$, all the curves for different temperatures collapse and the flux becomes independent of kT for a given value of $\varepsilon_{fw}^2/(kTF_e\sigma_{fw})$. In this regime, ε_{fw} is more important than kT. Between the two regimes is the transition regime, where the flux changes from ε_{fw} independent to kT independent. It has to be pointed out that the three regimes are undetectable if the flux is plotted versus ε_{fw}/kT.

The comparison between the behaviors of the flux for Ar and He indicates the role of the fluid-fluid self-binding energy ε_{ff} that lies in the regime of strong surface effect, where $\varepsilon_{fw}^2/(kTF_e\sigma_{fw})$ is large and fluid adsorption occurs. If ε_{ff} is comparable to the temperature, ε_{ff} can enhance the effect of temperature, as indicated by the temperature dependent flux for Ar (Fig. 1). If ε_{ff} is much smaller than the temperature, the fluid-fluid interaction has little contribution in freeing the fluid molecules from the adsorbed layers and the temperature effect seems to be less important compared to the strong surface effect.

Since the channel size is not involved in the dimensionless number $\varepsilon_{fw}^2/(kTF_e\sigma_{fw})$, it is necessary to examine the effect of channel size on the flow regimes observed in Figs. 1 and 4. Figures 5 and 6 depict the fluxes of liquid Ar and He in 1.8 and 2.8 nm channels. It is seen that the flow regimes observed in Figs. 1 and 4 remain unchanged. The effect of

channel size lies in the sensitivity of the flow to the temperature. It is easy to find that the flow is more sensitive to the temperature in small channels than large channels. For instance, the ratio of the reduced flux at 300 K to that at 100 K for $\varepsilon_{\mathrm{fw}}^2/(kTF_e\sigma_{\mathrm{fw}})\sim 100$ in Fig. 1(c) is 2.1, while this ratio is 4.1 in Fig. 5(a). This indicates that the flow behavior may become temperature independent and the flow regimes disappear when the channel size is larger than a critical value, where the classical theory may apply. This requires further explorations and is beyond the scope of current work.

We have summarized the flow regimes in Fig. 7. For small $\varepsilon_{\mathrm{ff}}/kT$, there are three flow regimes. As $\varepsilon_{\mathrm{fw}}^2/(kTF_e\sigma_{\mathrm{fw}})$ increases, the flux undergoes a transition from $\varepsilon_{\mathrm{fw}}$ independent (kT dominates) to kT independent ($\varepsilon_{\mathrm{fw}}$ dominates). If $\varepsilon_{\mathrm{ff}}/kT\sim 1$, the critical value of $\varepsilon_{\mathrm{fw}}^2/(kTF_e\sigma_{\mathrm{fw}})$ divides the flow into weak and strong fluid-wall interaction regimes. In the weak-interaction regime, the fluid flux decreases as the temperature increases, while the fluid flux is enhanced when the temperature is raised in the strong-interaction regime, as illustrated in Fig. 7. Finally, it is worth mentioning that the external forces, in the current work, are relatively small. If the external force is large, the fluid heating due to different sources of friction can be important [3]. In this case, whether the heating effect can be incorporated into the temperature requires further investigation.

This work was supported in part by the Hong Kong Innovation and Technology Fund under Grant No. GHP/035/07GD and the University Initiative Grant No. SBI07/08.EG01.

[1] Z. Li and H. Wang, Phys. Rev. Lett. **95**, 014502 (2005).
[2] Z. Li and G. Drazer, Phys. Fluids **18**, 117102 (2006).
[3] Z. Li, Phys. Rev. E **79**, 026312 (2009).
[4] R. S. Voronov, D. V. Papavassiliou, and L. L. Lee, J. Chem. Phys. **124**, 204701 (2006).
[5] U. Heinbuch and J. Fischer, Phys. Rev. A **40**, 1144 (1989).
[6] P. A. Thompson and S. M. Troian, Nature (London) **389**, 360 (1997).
[7] N. V. Priezjev, Phys. Rev. E **75**, 051605 (2007).
[8] A. Martini, H. Hsu, N. A. Patankar, and S. Lichter, Phys. Rev. Lett. **100**, 206001 (2008).
[9] Z. Li and L. Hong, J. Chem. Phys. **127**, 074706 (2007).
[10] I. Bitsanis, J. J. Magda, M. Tirrell, and H. T. Davis, J. Chem. Phys. **87**, 1733 (1987).
[11] P. A. Thompson and M. O. Robbins, Phys. Rev. A **41**, 6830 (1990).
[12] J. Koplik, J. R. Banavar, and J. F. Willemsen, Phys. Fluids A **1**, 781 (1989).
[13] M. Sun and C. Ebner, Phys. Rev. Lett. **69**, 3491 (1992).
[14] K. P. Travis, B. D. Todd, and D. J. Evans, Phys. Rev. E **55**, 4288 (1997).
[15] K. P. Travis and K. E. Gubbins, J. Chem. Phys. **112**, 1984 (2000).
[16] J. L. Barrat and L. Bocquet, Phys. Rev. Lett. **82**, 4671 (1999).
[17] M. Cieplak, J. Koplik, and J. R. Banavar, Phys. Rev. Lett. **86**, 803 (2001).
[18] T. M. Galea and P. Attard, Langmuir **20**, 3477 (2004).
[19] H. Takaba, Y. Onumata, and S. Nakao, J. Chem. Phys. **127**, 054703 (2007).
[20] C. Huang, P. Y. K. Choi, K. Nandakumar, and L. W. Kostiuk, J. Chem. Phys. **126**, 224702 (2007).
[21] C. Y. Soong, T. H. Yen, and P. Y. Tzeng, Phys. Rev. E **76**, 036303 (2007).
[22] N. V. Priezjev, J. Chem. Phys. **127**, 144708 (2007).
[23] H. Hippler, J. Troe, and H. J. Wendelken, J. Chem. Phys. **78**, 6709 (1983).
[24] M. P. Allen and D. J. Tildesley, *Computer Simulation of Liquids* (Oxford, New York, 1987).
[25] In this regime, the adsorbed molecules form sticky molecular layers, which do not take part in the flow. For the case shown in Fig. 1, there is only one layer of sticky molecules when $\varepsilon_{\mathrm{fw}}^2/(kTF_e\sigma_{\mathrm{fw}})\sim 100$. If $\varepsilon_{\mathrm{fw}}^2/(kTF_e\sigma_{\mathrm{fw}})\sim 10^4$, there are about two sticky molecular layers. Similar results were found in Ref. [5].